McKelvey School of Engineering Theses & Dissertations

McKelvey School of Engineering

Fall 12-21-2022

Effect of Diabetes-associated Mutations in Kir 6.2/Sur1 on KATP Channel Activities

Yunpeng Li
Washington University in St. Louis

WASHINGTON UNIVERSITY IN ST. LOUIS

McKelvey School of Engineering
Department of Biomedical Engineering

Thesis Examination Committee:
Colin Nichols, Chair
Sunjoo Lee
Maria Remedi
Jonathan Silva

Effect of Diabetes-associated Mutations in Kir 6.2/Sur1 on KATP Channel Activities
by
Yunpeng Li

A thesis presented to
the McKelvey School of Engineering
of Washington University in
partial fulfillment of the
requirements for the degree
of Master of Science

December 2022
St. Louis, Missouri

Table of Contents

List of Figures

List of Tables

<u>Acknowledgments</u>

ABSTRACT OF THE THESIS

Effect of Diabetes-associated Mutations in Kir 6.2/Sur1 on KATP Channel Activities

by

Yunpeng Li

Master of Science in Biomedical Engineering

Washington University in St. Louis, 2022

Professor Colin Nichols, Chair

Maturity Onset Diabetes of the Young (MODY) is a type of diabetes, distinct from either type I or type II, that happens before age 25 (MedlinePlus, 2022). Unlike the other two more common forms of diabetes, MODY is classified as a series of monogenetic disorders (American Diabetes Association Professional Practice Committee, 2021), caused by autosomal mutations. MODY is typically characterized by insufficient secretion of insulin, a similar symptom to type I diabetes, classified into 14 different types based on mutations found on different genes. Among them, subtypes 12 and 13, also called neonatal diabetes mellitus (NDM), are caused by gain-of-function mutations in Kir6.2 or SUR1, subunits of ATP-sensitive potassium (K_{ATP}) channels, and result from overactive K_{ATP}-driven loss of insulin secretion.

K_{ATP} channels are a type of potassium channels that are gated by the concentration of intracellular ATP and ADP, and consist of tetramers of inward-rectifier potassium channel (Kir6.x) subunits, surrounded by 4 regulator sulfonylurea receptors (SUR) subunits. They are widely found in human tissues, including cardiac, brain, skeletal muscles, smooth muscles, pancreas, and neurons. K_{ATP} channel function in pancreatic β-cells was first described in 1984 in rat pancreas islets. In contrast to NDM, congenital hyperinsulinism (CHI) results from loss of function of K_{ATP} channels, which leads to hypersecretion of insulin. However, clinical data show

that CHI patients frequently experience a transition from hypersecretion of insulin to a high blood glucose level, although there are few previous studies that highlight this transition, and the nature of the ensuing diabetes is unknown.

Our collaborators in India have identified a large number of NDM and CHI patients, but also a number of patients diagnosed with MODY, but not NDM, and harboring K_{ATP} channel mutations. The goal of this study was to analyze the functional consequences of the associated K_{ATP} mutations, in order to shed light on the mechanisms underlying the resultant diabetes.

In this project, I used fluorescence-based $Dibac_4(3)$ and thallium flux assays to investigate the effect of mutations on channel expression and function. The signals captured by these two assays illustrate the activities of mutated channels, reflecting the channel conductance. From the results, it is clear that the MODY-associated mutants are expressing loss of function behaviors. In particular, G163S and R1436P in SUR1 generate no channel activity, even after channel activators are applied to the cells. The results are not consistent with the idea that these MODY patients suffer from MODY 12 and 13 (i.e. NDM), but instead suggest that they should suffer from hypersecretion of insulin. Thus, the reasons for high blood glucose level in these MODY patients is unclear. It is possible that these patients are all CHI patients who have experienced a crossover from hyperinsulinism to diabetes, potentially explaining why K_{ATP} inhibitor therapy is unsuccessful in them. The mechanism of the transition process remains unclear, providing a future research direction to assess the transition mechanism, as well as pointing to a new sub-classification of MODY.

Chapter 1: ATP-sensitive potassium channel

1.1 Introduction to ATP-sensitive potassium channel

Bioelectrical activities are critical in all living organisms - they support the basic functions of life. Ionic potentials are maintained by the activities of sodium, potassium, calcium, and chloride channels (Nichols et al., 2006). Altered balance of channel open and closed states leads to differences of membrane potential, when the membrane potential reaches the threshold, generating action potentials which give signals to control cellular activities. Thus, there are multiple types of channels that are in control to the regulation of the membrane potential such as voltage-gated Na^+, Ca^{2+} and K^+ channels.

Of the multiple ion channels that are in control of electrical activity, ATP-sensitive potassium channels (K_{ATP} channels) are uniquely metabolically-sensitive channels that were firstly defined through ATP intracellular injection into energy-limited cardiac cells in 1983 by Noma et al. They treated the cardiac cells with cyanide to mimic hypoxia and lower the cytoplasmic energy, and then reported that injecting intracellular ATP closed the channels in patch clamp experiments (Noma et al., 1983). Subsequently, similar ATP-sensitive potassium channels were reported in many other tissues (Tinker et al., 2013).

K_{ATP} channels are composed of four inward-rectifier (Kir6.x) subunits associated with four sulfonylurea receptors (SUR), Four genes have been identified: ABCC8 which codes for SUR1 and KCNJ11 which codes for Kir6.2 are located on human chr11p15.1, ABCC9 which codes for SUR2 and KCNJ8 which codes for Kir6.1 are located on human chr12p12.1. Mutations in K_{ATP} channel genes lead to various diseases such as Cantu Syndrome (Grange et al., 2019), neonatal diabetes and others (Konganti et al., 2015).

1.2 Tissue Distribution and Physiological Function

K_{ATP} channels are widely expressed on the plasma membrane in brain, cardiac, vascular, skeletal and smooth muscles, pancreas and neurons (Seino et al., 2003). When outside energy sources, such as carbohydrates or lipids are absorbed by the human body, they will be transformed into ATP that can be utilized by cells. On K_{ATP} channels, there are binding sites for high energy ATP as well as for ADP, which play an antagonist role in the channel gating process, the open and closed states of K_{ATP} channels depending on the ratio of intracellular ATP and ADP. When the ratio is increased, more ATP will bind to Kir6.x subunits and the channel will be inhibited. Conversely, when the ratio is decreased, ADP binding to the ADP binding cassette on SUR subunits will activate the channel to an open state (Fig 1).
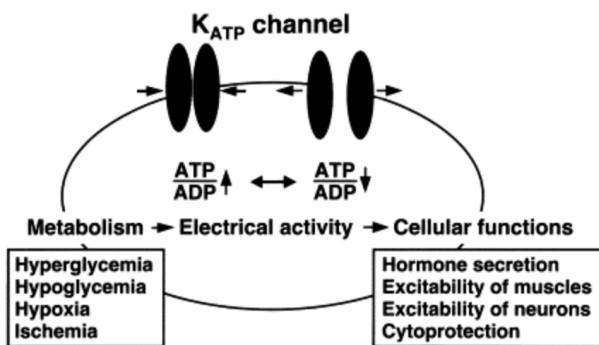
Seino S et al (2003). Prog Biophys Mol Biol 81(2):133-76.

Figure 1. The gating process of K_{ATP} channels is controlled by the ratio of intracellular ATP/ADP. The activation of K_{ATP} channels is involved in various metabolic and electrical activities, and cellular functioning.

1.3 Channel structure

K_{ATP} channel are hetero-octamers composed of a potassium channel subunit tetramer (Kir6.x) associated with four SUR subunits which belongs to the ATP-binding cassette (ABC) family of transporters (Vedovato et al., 2015) (Fig 2). There are potassium ion binding sites at the entrance of the Kir6.x subunit-generated potassium channel pore. The nucleotide binding domains at the intracellular side of SUR subunits are the domains for MgADP binding, which is responsible for channel opening. ATP binds to a binding pocket on the cytoplasmic side of Kir subunits and leads

to closure K_{ATP} channels, which is antagonized by MgADP binding to SUR. Thus, the opening or closing of the channels mainly depends on the balance of intracellular ATP and MgADP.
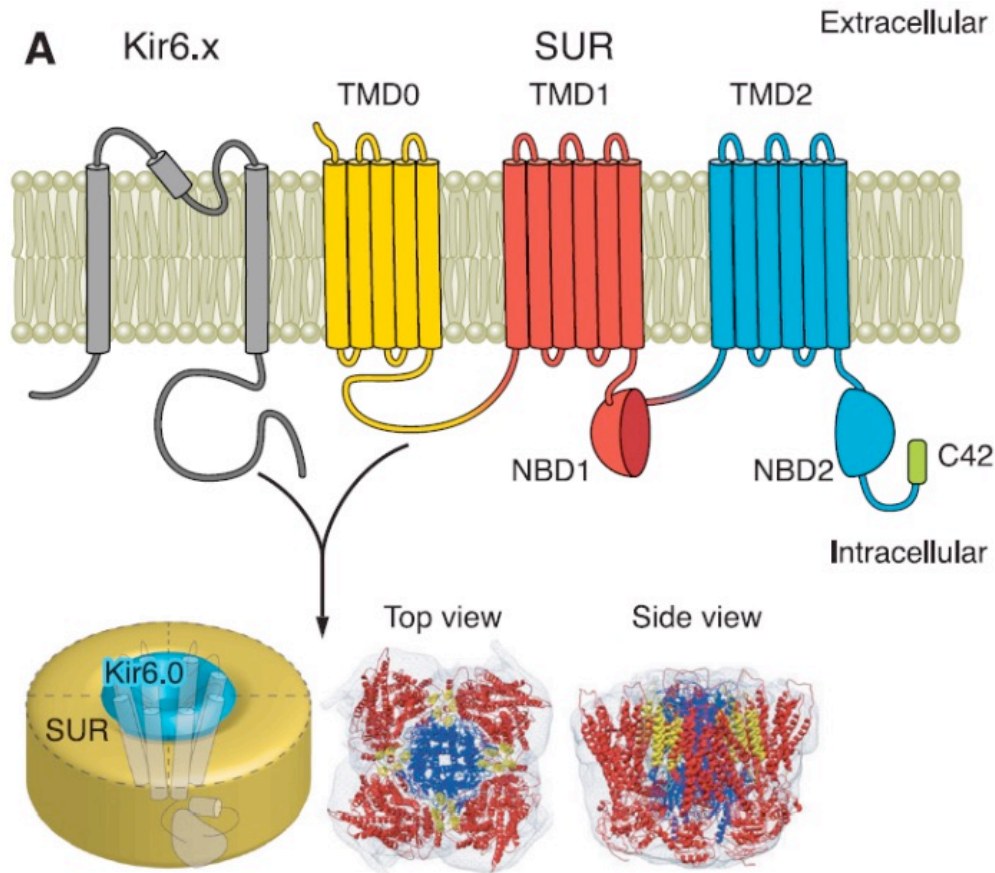
Hibino et al., 2010

Figure 2. Structure of K_{ATP} channel. Hetero octamer complex of K_{ATP} channel. Kir6.x subunits are located in the inner ring of the complex, encoding for the channel pore; four SUR subunits are surrounded outside of the Kir6.x subunits. Each Kir6.x subunit has four potassium ion binding sites at the entrance of the pore, both N-terminus and C-terminus are at intracellular side. The SUR subunits has three transmembrane domains (TMD0, TMD1 and TMD 2), and two nucleotide binding domains (NBD1 and NBD2), N-terminus is at extracellular side and C-terminus is at intracellular side.

1.4 K_{ATP} channels are involved in diabetes and other insulin related diseases

The importance of K_{ATP} channels in insulin secretion has been established by studies on

pancreatic β cells in the islets of Langerhans (Saint-Martin, 2011), which indicate the

relationship between membrane permeability to potassium and glucose induced membrane

depolarization (Ashcroft et al., 1984). Congenital Hyperinsulinism (CHI) and Neonatal Diabetes Mellitus (NDM), are two distinct diseases, the first due to loss of function (Loechner et al., 2010), the other due to gain of function of K_{ATP} channels (Yan et al., 2022), resulting from missense mutations in K_{ATP} channels in pancreatic islets β cells and are inheritable from parents.

Glucose is the main energy source within the blood and determines the metabolism level in β-cells. When there is low plasma glucose, intracellular metabolism level is low, the intracellular ATP/MgADP ratio decreases, leading to opening of K_{ATP} channels. Membrane potential will stay at the resting level of about -70mV and there will be no insulin release triggered (Fig 3A). When plasma glucose is raised, the decomposition of glucose produces ATP, which raises the intracellular ATP/MgADP ratio and closes the K_{ATP} channels. The membrane is now depolarized, triggering the opening of voltage-gated calcium channels. Calcium ions flow into the cells and trigger the secretion of insulin stored in the pancreatic cells (Fig 3B). When gain of function (GOF) happens in the Kir6.2/SUR1 subunits, as found in neonatal diabetes (NDM) patients, the K_{ATP} channel will be insensitive to the inhibition effect of ATP, the membrane thus stay hyperpolarized, and there will be inhibition of insulin release (Fig 3C); when loss of function (LOF) happens in the Kir6.2/SUR1 subunits, the channel activity will be reduced and cause a continuous depolarization. In this case, calcium channels will tend to stay opened, and continuously trigger the hypersecretion of insulin (Ashcroft et al., 2005). This situation is typically found in congenital hyperinsulinism (CHI) patients (Fig 3D).

A — Plasma glucose low
No insulin release
Metabolism low
Decreased ATP
Increased MgADP
K⁺
K$_{ATP}$ channels open
−70 mV
Ca²⁺ channels closed
Membrane hyperpolarized
Low metabolism
K$_{ATP}$ channels open
Less insulin secreted

B — Plasma glucose high
Glucose
Insulin release
Metabolism high
Increased ATP
Decreased MgADP
Ca²⁺
K$_{ATP}$ channels closed
Ca²⁺ channels open
Depolarization
High metabolism
K$_{ATP}$ channels closed
Insulin secreted

C — Gain-of-function-mutations in Kir6.2
Glucose
No insulin release
Metabolism high
Increased ATP
Decreased MgADP
K⁺
K$_{ATP}$ channels insensitive to ATP, so remain open
Membrane hyperpolarized
Ca²⁺ channels closed
K$_{ATP}$ channels more open
Less insulin secreted
Neonatal diabetes

D — Loss-of-function-mutations in SUR1 and Kir6.2
Insulin release
Ca²⁺
No functional K$_{ATP}$ channels
Ca²⁺ channels open continuously
Depolarization
K$_{ATP}$ channels closed
Insulin secretion unregulated
Congenital hyperinsulinemia

Ashcroft F. M. (2005). *The Journal of clinical investigation*, *115*(8), 2047–2058.

Figure 3. K$_{ATP}$ channels involved in insulin releasing mechanism, triggered by glucose traveled into the cells.
A. A start state of pancreatic cell, when blood glucose is low, there will be not much ATP generated, MgADP is playing a main role here, so K$_{ATP}$ channel is not inhibited by ATP thus membrane stays hyperpolarized. The resting potential is -70mV, there is no calcium ion getting through voltage-gated calcium channel thus insulin is not released. **B.** When blood glucose is high, there will be more ATP generated in the cell and tend to bind on Kir binding pocket to inhibit opening of the channel. Potassium stopped efflux and membrane potential decreases and the membrane is depolarized. In this case, voltage-gated calcium channel is stimulated and initiate calcium influx. When calcium ions getting in, they will send the signal and stimulate insulin secretion as a second messenger. **C.** An example of NDM, and **D** is an example of CHI.

1.4.1 Neonatal Diabetes Mellitus (NDM)

NDM is a rare form of diabetes that can be misdiagnosed as type I diabetes and, in most cases,

occurs in the first 6 months of life (De Franco et al., 2020). It is caused by gain of function of

K_{ATP} channels in pancreas islet cells through reducing ATP inhibition or enhancing MgADP activation (Ashcroft et al., 2017), leading to the hyperpolarization of the membrane, closure of voltage-gated calcium channels and inhibition of insulin secretion. Previously requiring injected insulin for therapy, sulfonylurea drugs, which inhibit K_{ATP} channels, can now be used to close the channels, reducing the pain of injections. Glibenclamide is a sulfonylurea that can be taken orally (Ashcroft et al., 2017) and can stimulate insulin secretion by closing the channels directly (Pipatpolkai et al., 2020). Orally taking glibenclamide has proved able to maintain euglycemia without injection of insulin and even more, the medicine may be stopped after a course of treatment and blood glucose may not bounce back (Şıklar et al.,2011). In one reported case, a 30-day male presented a stable normal blood glucose level after gradually reducing dosage of glibenclamide until 5 months and, at 8 months, completely stopped medication (Şıklar et al.,2011). Thus, compared to life-long injecting of insulin, orally taking glibenclamide can not only reduce the pain of injection, but also cut down the reliance on the medicine.

1.4.2 Congenital Hyperinsulinism (CHI)

CHI is another monogenetic disease, caused by loss of function of K_{ATP} channels, with the opposing phenotype – hypersecretion of insulin and hence low blood glucose. This type of condition is also typically identified in neonates (Boodhansingh et al., 2019). Loss of function of K_{ATP} channels was first discovered in 1995 (Thomas et al., 1995), the mechanisms including preventing channel trafficking onto the membrane surface, impairing the binding abilities of MgADP on SUR subunits (Nichols et al., 1996). Diazoxide, which activates K_{ATP} channels, is used as a major treatment for CHI, it has been found effective with KCNJ11 missense mutations and some ABCC8 mutations (De Franco et al., 2020).

Chapter 2: Maturity Onset Diabetes of the Young (MODY)

2.1 Introduction to MODY

Maturity Onset Diabetes of the Young (MODY) describes a group of diabetes conditions that happen typically before 25, characterized by above normal blood sugar levels (MedlinePlus, 2022), with decreased insulin release from the pancreas, so that glucose remains in the blood rather than being absorbed by cells. It is a genetic disease, caused by mutation of several genes (Table 1). MODY is usually identified at age of adolescence or early adulthood and is distinct from the common type I and type II form of diabetes. In the United States, up to 2% of MODY cases are diagnosed in adolescents of 20 or younger (Pinto et al., 2021). It is caused by single gene mutations and in genes that are expressed in pancreatic β cells and involved in insulin secretion and releasing process.

MODY is basically divided into types 1 to 14 based on mutated genes (Horikawa, 2018): GCK, HNF1A, HNF4A, HNF1B, INS, NEURO1, PDX1, PAX4, ABCC8, KCNJ11, KLF11, CEL, BLK, and APPL1 (Table 1). Type 12 and 13 are NDM caused by ABCC8 or KCNJ11, discussed above.

Subtype	MODY gene	Gene function	Pathophysiology	Other features	Treatment
MODY 1	*HNF4A*	Transcription factor	ß-cell dysfunction	Hyperinsulinism during infancy, low triglyceride level	Sulfonylureas
MODY 2	*GCK*	Enzyme in the first step of glucose metabolism	ß-cell dysfunction	Mild fasting hyperglycemia	No medications, diet
MODY 3	*HNF1A*	Transcription factor	ß-cell dysfunction	Glycosuria	Sulfonylureas
MODY 4	*PDX1*	Transcription factor	ß-cell dysfunction	Pancreatic agenesis in homozygote/compound heterozygote	Diet or OAD or insulin
MODY 5	*HNF1B*	Transcription factor	ß-cell dysfunction	Renal anomalies, genital anomalies, pancreatic hypoplasia	Insulin
MODY 6	*NEUROD1*	Transcription factor	ß-cell dysfunction	Neonatal diabetes, neurological abnormalities in homozygote	OAD or insulin
MODY 7	*KLF11*	Transcription factor	ß-cell dysfunction	Similar to type 2 diabetes	OAD or insulin
MODY 8	*CEL*	Controls exocrine and endocrine functions of pancreas	Pancreas endocrine and exocrine dysfunction	Exocrine dysfunction, lipomatosis	OAD or insulin
MODY 9	*PAX4*	Transcription factor	ß-cell dysfunction	Possible ketoacidosis	Diet or OAD or insulin
MODY 10	*INS*	Encode the proinsulin precursor	Insulin gene mutation	PND	Diet or OAD or insulin
MODY 11	*BLK*	Tyrosine kinase functions in signal transduction	Insulin secretion defect	Overweight	Diet or OAD or insulin
MODY 12	*ABCC8*	Regulating insulin release	ATP-sensitive potassium channel dysfunction	PND, TND	Sulfonylurea
MODY 13	*KCNJ11*	Regulating insulin release	ATP-sensitive potassium channel dysfunction	Neonatal diabetes in homozygote	OAD or insulin
MODY 14	*APPL1*	Insulin signal pathway	Insulin secretion defect	Dysmorphic phenotype, developmental delay	Diet or OAD or insulin

MODY, maturity-onset diabetes of the young; OAD, oral antidiabetic agents; PND, permanent neonatal diabetes; TND, transient neonatal diabetes.

Yeungnam Univ J Med 2020;37(1):13-21.

Table 1. Table of 14 subtypes of MODY found on different genes, and their clinical characteristics of gene function, pathophysiology, features, and associated treatments. MODY 12 found mutations on ABCC8 gene and MODY 13 found on KCNJ11 gene are involved in ATP-sensitive potassium channel (K_{ATP} channel) construction and functioning, mutations happen on these two genes will lead to dysfunction of K_{ATP} channel in pancreas β-cells and result in insulin releasing irregulating.

2.2 Appearance of an unexplained MODY phenotypes with KATP mutations

Although classified as Type 12 and 13 MODY, NDM, caused by gain of function mutations in

ABCC8 or KCNJ11, is present from birth, and typically diagnosed in the neonatal period, rather

than late childhood or early adulthood, as discussed above.

Our collaborators, Dr. Radha Venkatesan and colleagues, have collated 16 diagnosed NDM patients, and 19 diagnosed CHI patients, all with K_{ATP} mutations, many of the mutations having been previously characterized as gain- or loss of function mutants, respectively. However, they have also identified 11 patients diagnosed with MODY, but not neonatal diabetes, yet who also harbor K_{ATP} mutations of unknown functional consequence (Table 2). Many of these patients have been treated with the sulfonylureas glipizide, with variable results. For non-diabetic or well-controlled diabetic humans, there should be less than 99 mg/dL in fasting blood sugar (FBS), 100 – 140 mg/dL in PPBS and 4% - 5.7% in HbA1c levels. Notably, the initial post prandial blood sugar (PPBS) of patients with MODY mutations are ranging from 204 mg/dL to 464 mg/dL, which is much higher than normal, and in many cases, repeated measures following initiation of glipizide treatments, there was little or no improvement.

In order to record the channels activities of these MODY-associated K_{ATP} mutations at the molecular level, I have collected the specific MODY mutations from our collaborators in India that are listed at Table 2: H36D, G163S, R519C, R519H, A758V, V849I, D897E, A1007T, R1352C and R1436P on ABCC8. After research on NCBI and mutation locations, I eventually confirmed the gene sequence reference is NM_000352.

2.3   The object of thesis: to understand the basis of MODY in a Cohort of patients with K_{ATP} mutations

Intriguingly, among the collected information of MODY patients, some of the mutations (D860H, A977T, V601I) have also been reported in CHI (Table 2), although the channel functional consequences have not previously been reported. Importantly, treatment of these individuals with the sulfonylurea gliclazide, did not obviously improve their blood glucose control (Table 2). On the opposites, Arg1352Cys, Arg1436Pro, Ala758Val and Gly163Ser also

show a very poor response to treatments. What is also worth mentioning is, patient with mutation H36D was experiencing a recurring high blood glucose recorded from 143mg/dL to 329 mg/dL in FBS, 303 mg/dL to 464 mg/dL in PPBS, the blood glucose level rising instead of lowering between the first and the third measures following initiation of treatments.

A.

S. No	Gene	Amino Acid	Nature of Mutation	Treatment	FBS(mg/dL)						PPBS(mg/dL)						HbA1C(%)						Remarks
1	ABCC8	Arg1352Cys	Novel	Gliclazide	252	237	185	165	168	149	261	320	228	223	257	175	8.6	7.8	10.3	10.1	8.2	_	_
2	ABCC8	Arg1436Pro	Novel	Gliclazide	316	206	182	188	104	140	392	377	264	244	181	165	7.2	10.4	9.8	9.9	8.4	9.6	_
3	ABCC8	Asp860His	Known - Uncharacterized	Gliclazide	293	236	172	130	143	133	275	214	202	200	195	_	10.8	8.5	8.2	7.9	7.3	_	Asp860His was reoprted in CHI patient (Bellanné-Chantelot (2010) J Med Genet 47, 752). But we saw it in MODY patient.
4	ABCC8	Ala977Thr	Known - Uncharacterized	Gliclazide	229	90	90	101	98	108	363	121	139	129	123	183	10	6	5.6	6.2	5.7	5.7	Ala977Thr was reoprted in CHI patient (Banerjee, et al., 2011). But we saw it in MODY patient.
5	ABCC8	Ala758Val	Novel	Vildagliptin	254	160	109	117	128	_	285	179	165	145	152	_	9.8	6.5	7.1	6.8	6.4	_	_
6	ABCC8	His36Asp	Novel	VOSO MF	143	110	329	106	_	_	303	124	464	115	_	_	13.7	6.1	_	_	_	_	_
7	ABCC8	Gly163Ser	Novel	Glycomet	201	125	175	_	_	_	322	264	250	_	_	_	8.9	9.8	8.7	_	_	_	_
8	ABCC8	Arg519His	Novel	Glimepiride and Metformin	329	110	106	_	_	_	464	124	115	_	_	_	6.1	_	_	_	_	_	_
9	ABCC8	Val849Ile	Novel	T.GLIMEPIRIDE + .VILDAGLIPTIN+METFORMIN + Insulin	208	_	_	_	_	_	391	_	_	_	_	_	10.9	_	_	_	_	_	_
10	ABCC8	Ala1007Thr	Novel	METFORMIN	90	95	_	_	_	_	106	_	_	_	_	_	5.8	_	_	_	_	_	_
11	ABCC8	Val601Ile	Known - Uncharacterized	Gliclazide	288	270	242	_	_	_	399	374	340	_	_	_	10.4	8.7	_	_	_	_	Val 601 Ile was reoprted in CHI patient (Kapoor et al., 2013). But we saw it in MODY patient.
12	ABCC8	Glu971Val	Known - Uncharacterized	OHA/ Insulin	106	69	116	142	_	_	204	88	183	_	_	_	6.1	6.4	5.1	_	_	_	_
13	ABCC8	Gly1009Ser	Known - Uncharacterized	OHA/ Insulin	_	_	_	_	_	_	_	_	_	_	_	_	_	_	_	_	_	_	_
14	ABCC8	Arg519Cys	Novel	_	_	_	_	_	_	_	_	_	_	_	_	_	_	_	_	_	_	_	_
15	ABCC8	Asp897Glu	Novel	Glimepride / Glycomet	_	_	_	_	_	_	_	_	_	_	_	_	_	_	_	_	_	_	_
16	ABCC8	Ala1472Thr	Known - Uncharacterized	OHA	_	_	_	_	_	_	_	_	_	_	_	_	_	_	_	_	_	_	_
17	ABCC8	Val84Ile	Known - Uncharacterized	OHA	_	_	_	_	_	_	_	_	_	_	_	_	_	_	_	_	_	_	_
18	KCNJ11	Arg347Ser	Novel	Insulin+ Glimepiride	109	102	124	174	143	155	219	156	196	199	183	154	6.1	6.1	6.4	7.2	7.8	7	_

B.

	Fasting blood sugar (FBS)	Post-Prandial Blood Sugar (PPBS)	Glycated hemoglobin (HbA1C)
Normal	Less than 99mg/dL	100mg/dL ~ 140mg/dL	4% ~ 5.7%
Prediabetes	100mg/dL ~ 125mg/dL	/	5.7% ~ 6.4%
Diabetes	Larger than 125mg/dL	Higher than 140mg/dL	Higher than 6.5%

Table 2. Blood sugar indices of MODY patients compared to blood sugar standards. A. FBS, PPBS and HbA1C level of MODY patients with certain mutations recorded as clinical data. The data were obtained among a four year range from 2018-2022. **B. The standard of blood sugar levels from normal to diabetes according to three different indices.** Fasting blood sugar (FBS) is the blood glucose value measured before breakfast the next day after 8-12 hours fasting. The normal level should be less than 99mg/deciliter. The second is post-prandial blood sugar (PPBS) is the blood glucose value measured half to one hour after a meal, which reflect the highest blood sugar level. This level should be between 100mg/dL to 140mg/dL for a non-diabetes person. The glycated hemoglobin (HbA1C) is the hemoglobin and glucose binding products in red blood cells and the level of HbA1C reflects the prolonged blood sugar level. The normal value for a healthy person should be around 4% to 5.7%.

The diagnosis of MODY is primarily based on the fact that it happens during late childhood or adulthood, and that it is neither type I nor type II diabetes. Thus, three possibilities may be proposed for the basis of MODY in patients with mutations in K_{ATP} channels (Fig 4):

(1) The mutations cause gain of functions of the K_{ATP} channels, and thus the patients should have been diagnosed as NDM as neonates but were somehow missed.

(2) The mutations are benign and do not affect the channel functioning.

(3) The mutation actually causes channel loss of function. In this case, the patients may have initially suffered from CHI and then somehow crossed over to under secretion of insulin.

By assessing channel function of the mutants, the above hypotheses can be specifically tested, and this is the goal of my research.
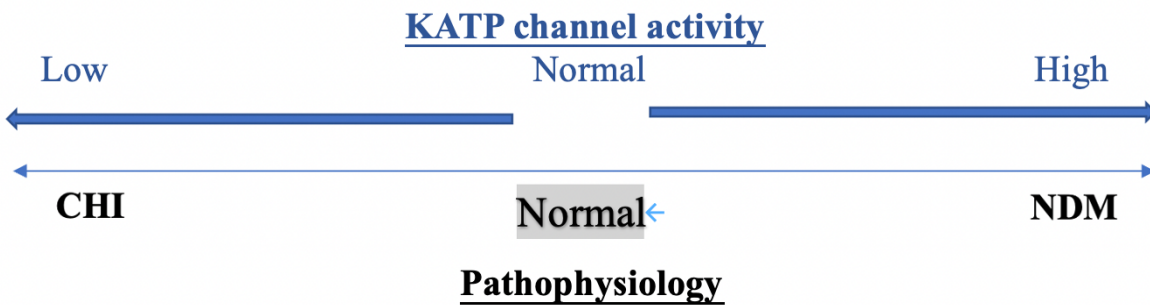

Figure 4. Relationship among CHI, Normal and NDM based on K_{ATP} activities.

Chapter 3: Methods, experimental process and results

3.1 Preparation for stable cell lines constructing

3.1.1 PCR of mutations

In this project, we are using Q5® High-Fidelity DNA Polymerases in PCR protocol produced from *Biolabs®*. This high-fidelity enzyme can make the correction based on 3'- 5' exonuclease activity, which can be 280 times higher than original *Taq* polymerase, as well as having a low error rate (Kommedal et al., 2012). It can also lower the requirement of CG content in both primer and template (*Biolabs®*, 2022).

The first part of plasmid construction is introducing mutations into human SUR1 (hSUR1) sequences. While designing primers for mutations collected from the MODY patients, we chose to design it into a 42 bp long primer for each mutation instead of designing a regular PCR primer of 20 bp long (Kommedal et al., 2012). The template plasmid (10k) sequence includes EcoRI and NheI restriction sites on the end of the hSUR1 clone. For the PCR protocol, each mutation correlates with a 50 ul PCR system, with 10 ul Q5 buffer, 10 ul Q5 enhancer, 1 ul dNTPs (10 mM), 2 ul DMSO, 0.5 ul Q5 polymerase, 1 ul template, 2 ul primer (1ul for each direction) and rest of the content is milli-Q® water. The PCR cycle starts from denaturing the template at 95 °C for 2.5 minutes, then annealing primers at 63 °C for 10 seconds, and extension at 72 °C for 8 minutes. Then the cycle is repeated for 25-30 times. After amplification, the products are kept at 4°C.

To check the PCR products are the right size, it is necessary to run an agarose gel electrophoresis. The mass concentration of agarose gel is 1 (g/ml) %, dissolved as powder in

TAE buffer, then microwaved for 2 alongside minutes. The liquid is set at room temperature to cool down for a while, then 1 ul/25 ml ethidium bromide, a small molecule for DNA illustration under UV light, is added. The samples are run with loading dye in 5:1 ratio for 20 min with 1 kb DNA ladder in a separat well.

If the bands are present at the corresponding location, 1ul DpnI is added to each sample, which will cut the methylated site on the template plasmid. Double strands PCR products that do not carry methyl are maintained. DNA Samples are stored in 37°C incubator for 2 hours or overnight.

3.1.2 Transformation

Mix the PCR product with E. coli at 1:5 ratio, before setting the mixture on ice for 30min. Then put the mixture in 42°C for 45 seconds, and quickly put it back on ice for 2 min. Add 200 ul SOC to each tube, which is a medium that contains the nutrients for microbial growth (SigmaAldrich et al., 2022), put them on 37°C shaker for 1 h. Centrifuge the mixture at 2000rpm speed for 2 min, discard 180 ul of upper liquid, mix the reminder well. Then overspread the mixture on the surface of LB solid medium which contains 1:1000 carbenicillin, of which effect can also be suppressed by the ampicillin resistance gene encoded in the template plasmid.

Culture the medium in 37°C incubator overnight.

The next day, pick two colonies from each medium and culture each colony in 7.5 ml liquid LB medium with 1:1000 carbenicillin in 50 ml EP tube. Put them in 37°C vortex table overnight.

3.1.3 Miniprep the plasmid

In this project, we are using QIAprep® Spin Miniprep kits (QIAPrep®, 2022). Centrifuge the EP tubes from previous steps for 5 min at 4200 rpm, then discard the liquid. Add 250 ul

resuspension buffer P1 into the EP tube and mix them well with pipetting to disperse the bacteria. Then add 250 ul lysis buffer P2 into the EP tube to break the cell membrane. Mix thoroughly. The mixture should turn blue. Then prepare 350 μl neutralization N3 buffer into a new 1.5 ml micro-centrifuge tube, which will neutralize the basic reagents from previous steps and adjust the solution into a higher salt concentration condition, prepare for binding next step. Transfer the content in EP tube into prepared N3, mix thoroughly until the solution becomes completely clear. Centrifuge the 1.5 ml tube for 10 min at 12000 rpm. Transfer 800 ul of supernatant into QIAprep spin column with a 2 ml collection tube, centrifuge the tube for 2 min at 12000rpm. Then add 500 ul binding PB buffer into the column in order to bind the double strand DNA onto the surface of spin column membrane, centrifuge for 2 min at 12000 rpm and discard the flow through. Add 750 ul wash PE buffer into the column to wash out extra remaining salt on the spin column membrane, centrifuge for 2 min at 12000 rpm and discard the flow through. Then centrifuge for another 1 min, discard the flow through. The last step is extracting DNA from the column. Transfer the column into a new 1.5 ml micro-centrifuge tube, add 50 ul elution buffer EB into the spin column, stay for 1min allowing PE buffer to volatilize, and centrifuge for 2 min at 12000 rpm. Discard the column and the flow through in 1.5 ml tube contains the plasmid DNA we want.

3.1.4 Sequencing

Send the plasmid DNA from the last step for sanger sequencing. Construct a 15 ul system with corresponding primer. The primer can walk through 800 bp long and should be at least 50 bp prior to the mutation sites to avoid fuzzy part in sanger sequencing.

3.1.5 Integrating mutations into attb vector

This vector should contain an attb sequence, which recognize the attp sequence in landing pad HEK293 cell (human embryo kidney 293 cells with Crispr induced sequences). Landing pad HEK293 is an improved carrier for gene expression by BxbI recombinase gene induced into attb vector (Matreyek, Stephany et al. 2020). After the attb on the vector recognizes attp on the genomic landing pad, the sequence on the vector will be able to integrate into the landing pad and promoted by Tet promoter contained on the landing pad sequence, which will be activated by doxycycline. Thus, while culturing the stable attp-attb stable cell lines, there should be doxycycline contained in the culturing media.

The other sequence needed to be included in the vector sequences are: T7, is the prompter which do not express in mammalian cells and allows the detection for Flag-tag; IRES, which can enhance the co-expression of two genes on a same vector (GeneCopoeia et al., 2022); NheI and EcoRI, restriction enzyme cutting sites; puromycin resistant sequence, which can be a selective marker while cells are cultured in the puromycin contained culturing media; and mCherry, red fluorescent gene to ensure the expression of the entire gene. The whole sequence should include as follows: (cycle) – T7 – attb— Mlu1 – hKir6.2— BglII – IRES – NheI — hSUR1— EcoRI — IRES— mCherry — puromycinR – (cycle). NheI and EcoRI should be on each side of hSUR1 in order to cut the original hSUR1 sequence out and replace it with the ones that contain the mutations. This part of PCR should integrate the two restriction enzymes recognizing sequences to each end of the insertion, and also a flag-tag sequence between NheI and the 5' end of the insertion. The primers used this time have two forward sequences, cutting the flag-tag sequence into two with overlapping sequences, one includes half of the flag-tag, which directly integrate onto the upstream insertion 5' end of DNA; the other includes the other half of the flag-tag and

15

the sequence of NheI. The third primer used is in the reverse direction in order to integrate the

EcoRI sequence into the other end of the insertion. Since the insertion is about 5 k long, change

the extension step of the PCR to 2.5 min and other steps keep the same.

3.1.6 Gel extraction

After running the agarose gel electrophoresis, cut the gel at where the correct bands present with

a gel extractor. Put the extractor into a 1.5 ml micro-centrifuge tube, centrifuge to gather the gel

at the bottom of the micro-centrifuge tube. Add 300 ul solubilization QG buffer into each tube.

Put the tubes in vortex table for 10min and set the temperature at 50°C until the gel completely

resolve in the QG buffer. If the solution stays yellow, which means the pH value is lower than

7.5, and is efficiency for DNA extraction. After the gel has completely resolved, add 100 ul

isopropanol into each tube to precipitate DNA since DNA is less soluble in isopropanol. Transfer

the solution into a QIAprep spin column with the collection tube, centrifuge the tube for 1min at

12000 rpm and discard the flow through. Add 650 ul wash PE buffer into each column to wash

out the extra salt, centrifuge for 1min at 12000 rpm, and discard the flow through. Centrifuge for

another 1min and discard the flow through. Then transfer the column to a new 1.5 ml micro-

centrifuge tube, add 30 ul elution buffer EB into each tube to extract the double strand DNA. Set

the tubes still for 1 min and centrifuge for 1 min at 12000 rpm. The flow through in micro tubes

is the DNA we need.

3.1.7 Ligase the insert into the vector

Construct a 20 ul system with 1 ul of NheI and EcoRI each, 2 ul of rCutSmart™ buffer

(*Biolabs®*, 2022), 5ul insert and 11 ul milli-Q® water, store in 37°C incubator 2 h or overnight, to

cut out the extra parts on the insert and cut the vector into two parts (5 k and 7 k). Run the vector

on an agarose gel and cut the 7 k part out from the gel. Do the gel extraction again to purify the

insert and extract the 7 k vector. Construct a 20 ul system with 2 ul ligase buffer, 1 ul ligase, 14 ul insert and 3 ul vector. Store it in a 4°C refrigerator overnight, to integrate the insert into the cut vector.

The transformation and min-prep process is the same as 3.1.2 and 3.1.3.

Construct a 20 ul system with 1 ug sample, 1 ul restriction enzyme KpnI, 2 ul of rCutSmart™ buffer and the rest of the content is milli-Q® water. Load the samples with the loading dye in 5:1 ratio, run the gel for about 20 min with 1kb DNA ladder. Send the samples that presents on the correct locations for Sanger sequencing.

3.1.8 Cell line construction

Digest the HEK293 with 200 ul trypsin, put the petri dish into the 37°C incubator for 2 min. Mix the solution thoroughly through pipetting a few times to make sure cells detached from the bottom of the petri dish. Transfer 25 ul of solution into each well of a flat bottom 48-wells plate, add 200 ul DMEM with 10% FBS and PS cell culture medium into each well, mix thoroughly but gently so won't harm the cells. Retain two drops of the cells for sub-culturing.

3.1.8.1 Transient cell line construction

We constructed cell lines for 10 mutations, 1 wild type and 1 for blank cells. The plasmids that do not contain attp-attb recombination recognizing site and BxbI recombinase sequence were used for transient transfection. In this case, we can carry out immediate experiments to assess channel activity.

Prepare two 1.5 ml PVC tubes, add 600ul opti-mem in each. Add 1.2 ug mCherry in the first tube, transfer 50ul into a new tube, add 3.3 ug hKir6.2 (in pcDNA3.1 -) into the remaining 550 ul of the mixture, mix thoroughly. Separate the mixture into 11 copies for the wild type and 10

mutations, add 500 ng hSUR1 (in pcDNA3.1 -) of the wild type or mutations to each tube. Then add 36 ul Fugene in to the second opti-mem tube, mix thoroughly. Wait for 5 min and transfer 53 ul of Fugene-Opti-mem mix to each of the tubes separated from the first mixture. Wait for 15-25 min and then drop the mixture onto the blank cells cultured on the 48-wells plate.

3.1.8.2 Stable cell line construction

The procedures for constructing stable cell lines are similar to the transient cell lines. However, we are using BxbI vector hence mCherry and hKir6.2 do not need to be added specially. So, we only need to apply attb and BxbI plasmid into the separated PVC tubes.

3.1.8.3 Passaging cells

Take out the petri dishes from 37°C incubator, add 200 ul trypsin and put the petri dishes back into the 37°C incubator for 2 min. After cells are digested, transfer two drops into a new petri dish, add 1.5 ml culture media and discard the old petri dishes.

3.2 DiBAC$_4$(3) Assay testing channel activities

3.2.1 DiBAC$_4$(3) Assay

DiBAC$_4$(3) is a small molecule with negative charge, it is fluorescent and can shuttle back and forth through the cell membrane according to the membrane potential (Adams et al., 2012). The molecular formula is $C_{27}H_{40}N_4O_6$ and its 2D structure is shown below (Fig 5). When the membrane is depolarized, it will enter cells and bind to intracellular protein or membrane and increase intracellular fluorescent intensity. When K_{ATP} channels are inhibited, the membrane will be depolarized, resulting in DiBac4(3) entering the cell and hence the fluorescence intensity will increase. Conversely, a higher fluorescent intensity indicates depolarization of the membrane, and lower channel activity. Thus, DiBAC$_4$(3) can be used to indicate the membrane potential and indirectly channel conductance.

18

This method is carried out in intact cells, in a condition which is similar to body environment, and measurements can be made very fast, with results of all mutations being available in a three-day period.
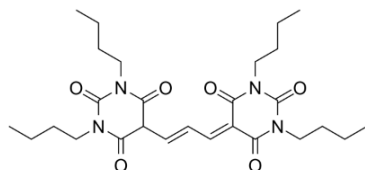

Figure 5. DiBAC₄(3) molecule structure

3.2.2 DiBAC₄(3) Assay protocol

Apply 80 ul poly-L-lysine into each well of a flat bottom 96-well plate by pipetting, in order to enhance the cell adhesion to the plate. Store in 37°C incubator overnight. Since we have 10 mutations as experimental group, 1 wild type and 1 blank cell as control groups, we basically designed each column for each type of cells. And designed each two wells in a column under the same condition of 100 nM glibenclamide, 10%MI, 100 μM diazoxide and a basal group.

Discard the poly-L-lysine solution. Transfer 4 ul of cells into a new petri dish after 200 ul trypsin digestion. Add 800 ul DMEM culturing medium with 1:5000 doxycyclin and 1:10000 puromycin, mix the solution thoroughly but gently. Apply 100 ul of the cells to each well on the 96-wells plate, store in 37°C incubator overnight.

From previous studies on medicinal effects, we decided to use glibenclamide to inhibit channel activity, and metabolic inhibitors (MI) and diazoxide as channel activators.

Prepare 100 nM glibenclamide, 10%MI and 100 μM diazoxide compounds before dealing with the 96-well plate, dissolve the compounds in 1mM K^+ solution to 2.4 ml with 3:1000 DiBAC₄(3) dye for each condition. The 1mM K^+ is composed of 139 mM of NaCl, 1 mM of KCl, 2 mM of

CaCl$_2$, 1 mM of MgCl$_2$, 10 mM of HEPES and 10 mM of glucose. This solution is similar to normal extracellular fluid. Use DMSO in basal group since it is the compounds storing solvent. Discard the culturing medium and wash the wells with 1mM K$^+$ solution two times and the third time use 3:1000 DiBAC$_4$(3) dye in 1 mM K$^+$ solution, by pipetting gently. Then apply the prepared compounds into each designed well and let the dye penetrate the cells for about 20 min. Scan the cells under fluorescent microscope under the blue light and red light, capture the photo under each condition for each well of cells. Since the cells express mCherry gene, the red fluorescent intensity will indicate the successfulness of transfection; the fluorescent intensity under blue light will indicate the channel activities and show up as green.

Analyze the photographs captured by fluorescent microscope with cell profiler, and quantify intensities. When capturing photographs, I used 10X lens. It is better to look for a field that includes as many cells as possible under red light, ensuring that the cells in the field have a high successful rate of transfection. The typical diameter is set for 20-60 in pixel units in the cell profiler, this range can help to exclude conspicuous spots of light coming from other small molecules and large clusters of cells.

3.3 Results

In this case, we planned to use Dibac$_4$(3) and thallium flux assay to assess channel activities perform under basal physiological conditions, as well as under maximally inhibited and maximally activated conditions. Glibenclamide and repaglinide are channel inhibitors that are often used in treatments of type II diabetes, diazoxide is clinically used channel opener in treating excessively secreted insulin in CHI. We expect Kir6.2/SUR1 channels will show a lower channel activity under channel inhibitor conditions and a higher channel activity under channel activator conditions.

3.3.1 Choices for appropriate compound and drug concentrations

We first tested glibenclamide, repaglinide, diazoxide, metabolic inhibitors and forskolin on control cells (with no K_{ATP} activity, transfected with Kir6.1 only) and K_{ATP} channel-expressing cells Kir6.2/SUR1.

Glibenclamide is one of the sulphonylurea agents that inhibit the K_{ATP} channel activities at the SUR subunit (Brayden et al., 2002). WT channels are sensitive to these agents at nano molar concentrations. Repaglinide is another K_{ATP} channel inhibitor which is secondly used in treating K_{ATP} channel disorders clinically. One of the effects of forskolin is recognized and utilized as K_{ATP} channel blocker at low dose (Hudman et al., 2000). Diazoxide is a clinically used channel activator. Control cells contained Kir6.1 but without a SUR subunit, so there is no channel activity. We first carried out a group of parallel experiments to analyze the effect on channel expression and opening of each reagent and combination of certain reagent (Fig 6).

We used 1 μM glibenclamide, 1 μM repaglinide, 100 μM diazoxide 100 μM forskolin and metabolic inhibitor in the first set of experiment, testing on both control and Kir6.2/SUR1 expressing cells.

Compared to the basal group, we showed that except for forskolin, both glibenclamide and repaglinide showed an inhibitory effect on Kir6.2/SUR1 channel (increased fluorescence, i.e. depolarization); diazoxide showed a channel activating effect on Kir6.2/SUR1 (decreased fluorescence, i.e. hyperpolarization) even in the presence of the inhibitor glibenclamide. However, MI did not show much channel activating effect whether directly applied or applied after glibenclamide on Kir6.2/SUR1 channels (Fig 6 orange). As expected, none of the compounds showed corresponding results on control cells.
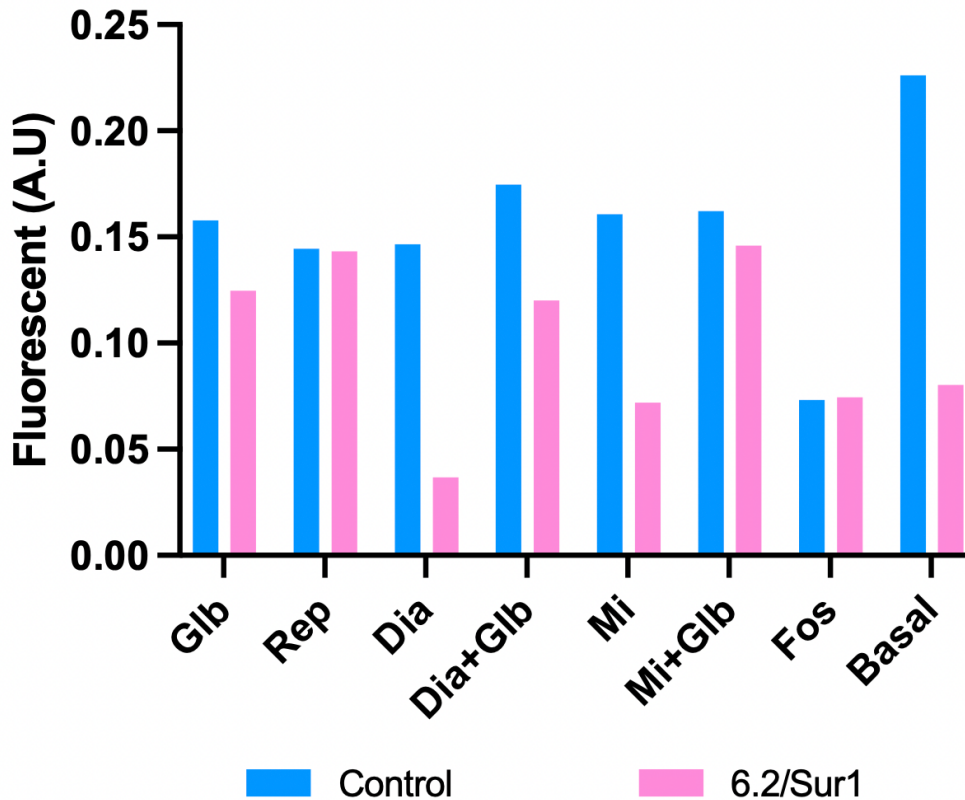
Intensities-Compounds

Figure 6. Detecting fluorescence intensity based on different compounds. Glibenclamide (Glb), repaglinide (Rep) and forskolin (Fos) are channel inhibitors, diazoxide (Dia) and metabolic inhibitor (MI) are channel activator. Compared to basal group, diazoxide has a better channel activating effect than metabolic inhibitors after the repression of glibenclamide on Kir6.2/SUR1.

Interestingly, while there is concentration dependent depolarization (increased fluorescence) at glibenclamide and repaglinide concentration between 10^{-4} nM to 100 nM, these reagents show hyperpolarization (decreased fluorescence) at concentrations of 10^{-4} nM to 10^{-5} nM, suggesting a potential channel activating effect, or perhaps activation of an intrinsic conductance in this range (Fig 7).
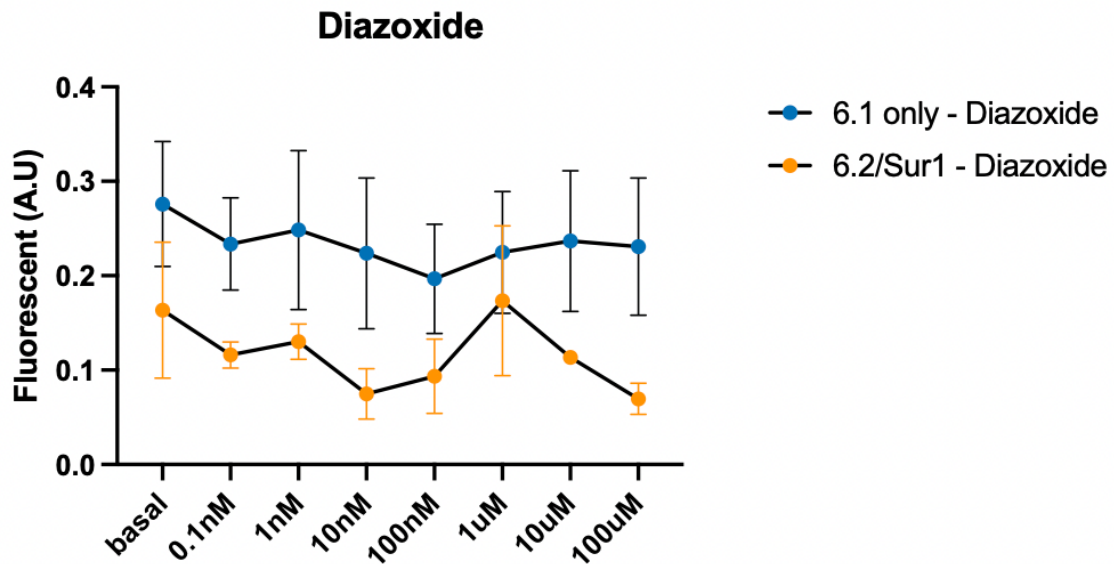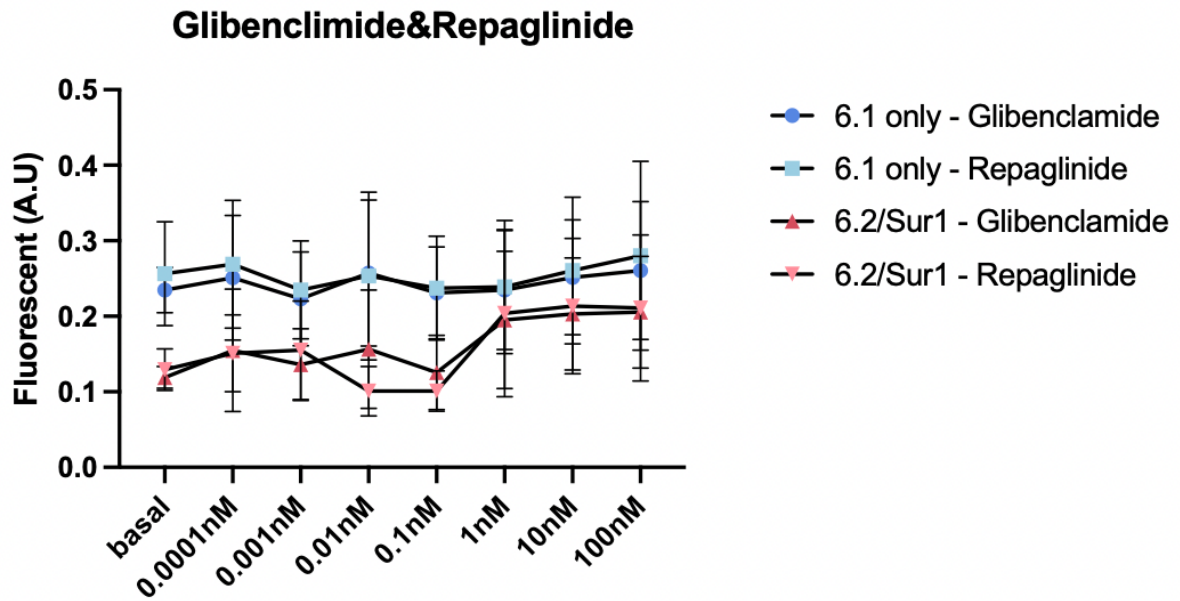
Figure 7. Average fluorescent intensities detected under different conditions. Upper. Average fluorescence intensities detected under 0.0001 nM – 100 nM glibenclamide and repaglinide (n=4). Both of glibenclamide and repaglinide showed the activating effect between 0.1nM to 0.001nM concentration range on Kir6.2/SUR1. **Lower. Average fluorescence intensities detected under 0.0001 nM– 100 μM diazoxide on both Kir6.1 (blue) and Kir6.2/SUR1 (orange) (n=4).** The channel opening effect are basically gradually decreasing as the concentrations

raising (except for 1 μM on Kir6.2/SUR1). The activating effect are appreciable under both 10 μM and 100 μM concentration and is the most obvious under 100 μM concentration on Kir6.2/SUR1.

Clear depolarization is seen for both glibenclamide and repaglinide at 1 nM, thus we tended to use this concentration in further MODY mutation channel activities examinations. In a test of the concentration dependence of diazoxide, we found that both 10 μM and 100 μM can lead to appreciable activating effect (hyperpolarization) on Kir6.2/SUR1 channels (Fig 7).

3.3.2 Testing the channel activities of transiently transfected cell lines with MODY mutations introduced into Kir6.2 and SUR1 in HEK293 cells

3.3.2.1 Dibac$_4$(3) Assay

We used the Dibac$_4$(3) assay to analyze the channel activities with mutations carried on SUR1 subunits under 1 nM glibenclamide, 10 μM diazoxide and metabolic inhibitors (Fig 8). With an initial hypothesis that prediction 1 is correct (i.e. that the MODY-associated mutations are causing gain of function), we expected mutations will activate the channel activities.

We initially attempted to assess channel activities with transient expression, but results were essentially uninterpretable (Fig 8). Since the control (blank) cells are not transfected with either Kir or SUR cDNAs, they were not expected to respond to any of the 4 conditions in this case, but the signals are as variable as the mutant signals, suggesting a significant experimental variability. In addition, both glibenclamide and diazoxide tended to cause hyperpolarizing signals, while MI caused an apparent depolarization.
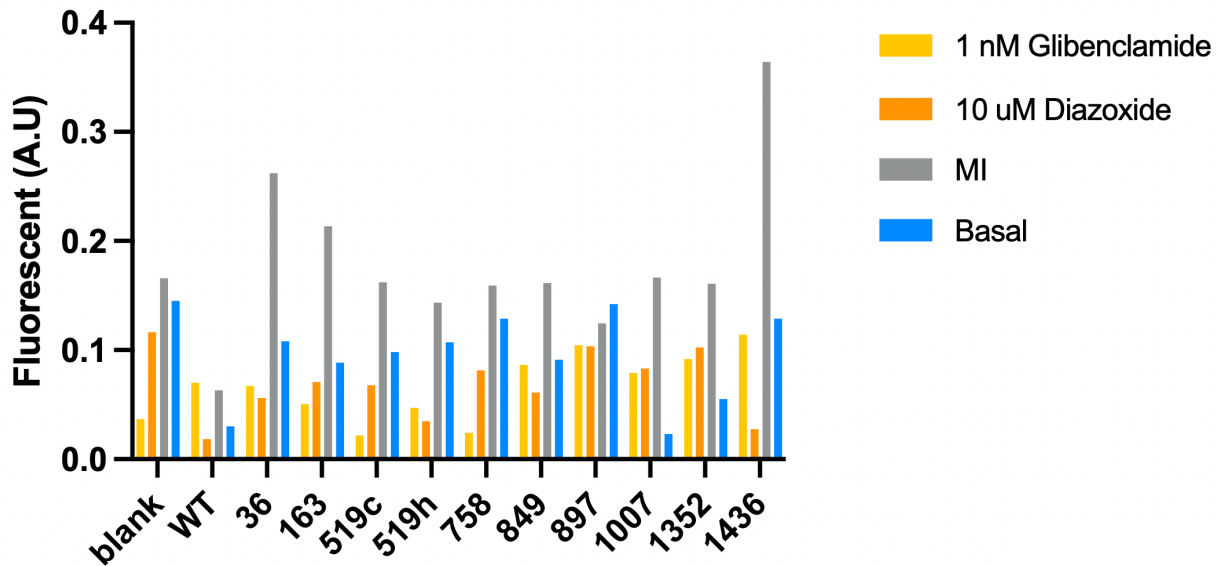
Figure 8. The influence of single mutations on SUR1 subunit on channel activities under channel inhibitor and activator conditions (n=4).

3.3.3 Testing the channel activities of stable cell lines with MODY mutations introduced into Kir6.2 and SUR1 in HEK293 cells

In order to maintain the inhibiting effect of glibenclamide, we increased the concentration to 100 nM. Since 100 μM diazoxide also showed an obvious activating result, we decided to switch the concentration to 100 μM this time. For metabolic inhibitors, we decreased its concentration to 10%, and assessed channel activities using the DiBAC4(3) Assay.

Using un-transfected landing-pad only (Blank) cells as a control group, there was a stable signal in the 4 conditions and wild type (human SUR1 + Kir6.2) signals changed as expected in the 4 conditions.

The level of fluorescent intensities in the blank cells illustrate the maximum depolarization of the membrane with no K_{ATP} channel expression (Fig 9A). Compared to the blank cells, wild type

showed a decrease in the basal fluorescent intensity, which means there is a channel activity under the controlling condition in WT.

The WT showed even more channel activities under the applications of both channel activators. In addition, 100 μM diazoxide showed more significant channel activating effect on WT. The channel activities under 100 μM of diazoxide indicate the maximum hyperpolarization of the membrane, under the assumptions of similar number of channel expression in both WT and mutants since they are all from the same batch of transformation.

When treated with 100 nM glibenclamide, WT fluorescent intensity reached about the same as blank cells, indicating that the channel activities are almost fully inhibited in this condition (Fig 9A).

Very interestingly, compared to the wild type, no mutation presented higher basal activity (i.e. hyperpolarization), and many showed much less or no activity. In mutations G163S, V897I and R1436P, there was a very high basal signal, and no effect of the channel opener, consistent with essentially no channel activities, comparable to the glibenclamide condition for mutations G163S and R1436P (Fig 9B). These results indicate a loss of channel function due to the mutations, essentially a complete loss in mutations G163S and R1436P, which is opposite to the hypothesis that these MODY mutations are similar to NDM mutations, characterized by gain of function. Even though both patient groups are diagnosed with high blood glucose.

A.

B.

Comparison among mutants
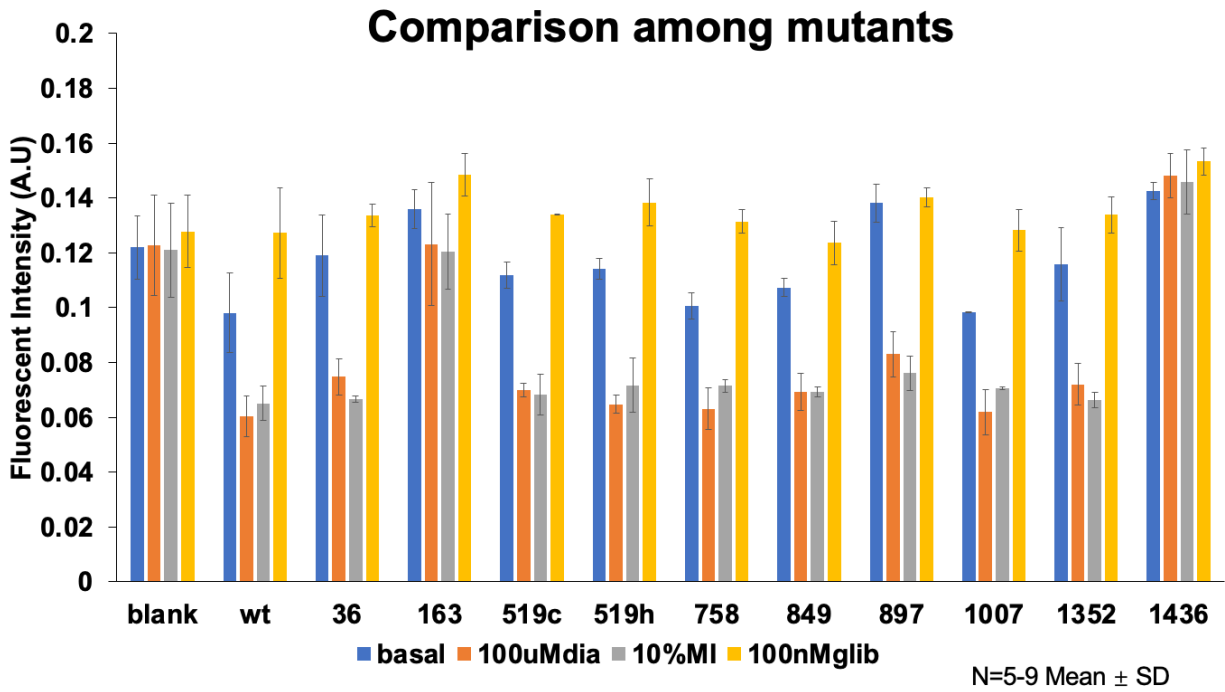
N=9 Mean ± SD

N=5-9 Mean ± SD
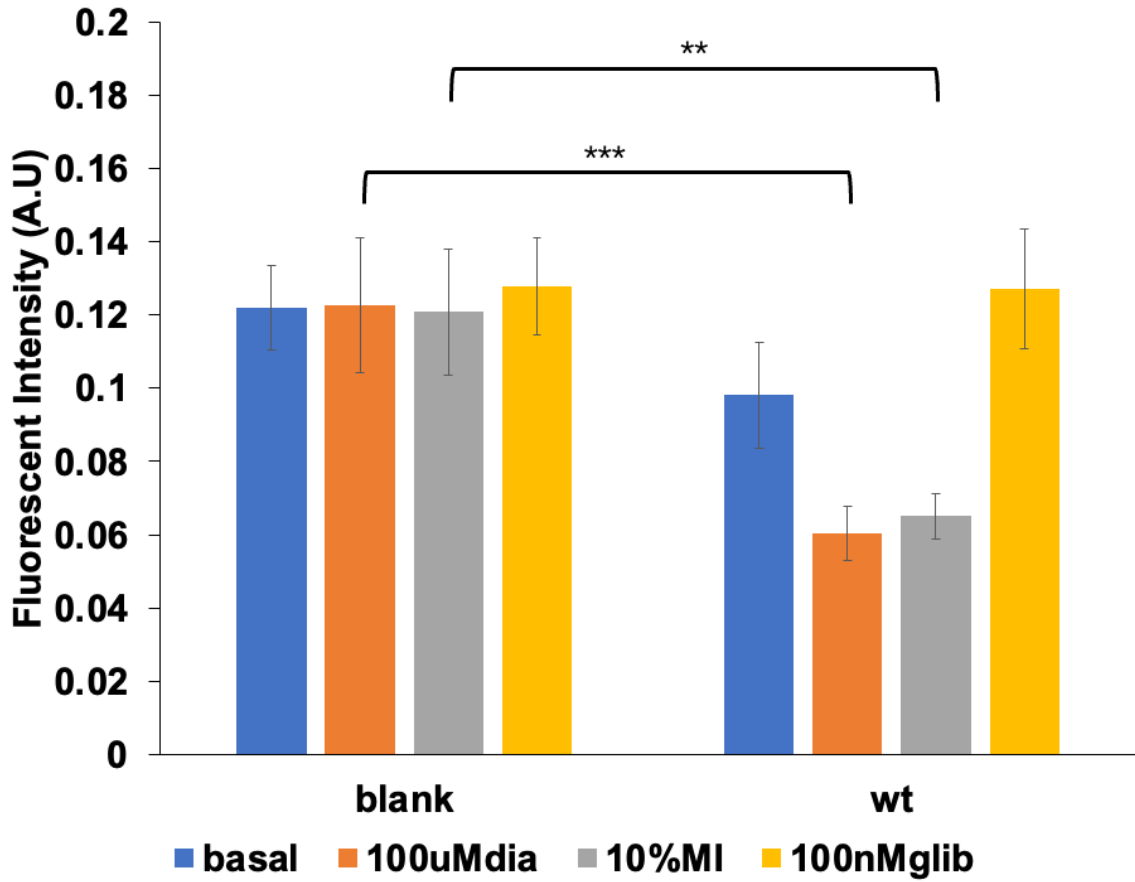
Figure 9. Fluorescent intensity. A. Dibac fluorescent of blank cells and WT (n=5-9). The difference between treatments after channel inhibitor and channel activators is distinctive compared from basal condition. Stars indicate the P-value analyzed by one-way ANOVA by Prism. More stars mean a smaller P-value, and more significant between two groups. **B. Dibac fluorescent indicating channel activities of mutations under different pharmacological treatments (n=5-9)**

Under the basal condition, all the mutants showed a higher intensity than wile type, which indicates the channel activities in mutants are lower than the wild type, and the K_{ATP} channels function may be lost. This indicates that these mutations are not causing MODY 12 and 13, which are recognized as neonatal diabetes caused by gain of functions on KATP channels. Particularly, G163S, D897E and R1436P showed a much higher intensity, reflecting an apparent almost complete loss of activity.

Under the condition of 100 μM diazoxide, nearly all the mutants showed a significant channel opening, except for G163S and R1436P. These two mutants showed a similar fluorescent intensity to the blank cells. This might have no response to the drug treatments.

The mutants showed a similar result under 10% MI condition to the 100 μM diazoxide. G163S and R1436P still have no response to the drug treatment. This can give us a possibility that there might be no channel expressing in these two mutants.

In 100 nM glibenclamide, channel activities are comparable to the blank cells and G163S and R1436P again, showed even higher fluorescent intensities to the blank cells.

3.3.4 Discussion and future directions

The results show that all of the mutations associated with a MODY diagnosis caused loss of function in K_{ATP} channels. Back to our predictions on how mutations may affect the channel activities, the results are not consistent with hypothesis 1, i.e. none of them caused gain of function. They are also not consistent with hypothesis 2, i.e. that the mutations were without

effect, and therefore not contributing to the phenotype. Instead, especially in mutations G163S and R1436P, there was no channel activity in any condition applied. These patients would thus be predicted to suffer from CHI, which has been shown to result from channel loss of function (Maiorana et al., 2014), and associated with hyperinsulinism during their life as infants; patients with NDM suffer from diabetes as neonatal life have been recorded with gain of function mutations (Remedi et al., 2009). Combining the clinical observation and experimental studies of these MODY-associated mutations, both loss of function of channel activities and high blood glucose are present. In this case, a new question has been brought out that the inconformity between the mutation induced channel behavior and blood glucose level in MODY patients, and suggests that these patients, rather than suffering from a subtle NDM, have transitioned from CHI to diabetes, as has been reported in isolated cases (Işık et al., 2019). This may bring us to recognize a new subtype of MODY, in which patients may have suffered from CHI during their infant period, and somehow transit into diabetes along with their growth to an elder age.

The results provide a future direction to work on. Other than the effects of channel inhibitors and activators, the efficiency for channels trafficking onto the membrane surface should be considered in further studies. G163S and R1436P have been shown similar channel behavior compared to the blank cells, which raises the possibility that there are trafficking defects as seen in some recognized CHI mutations (Kharade et al., 2016), with no channel expressing in the cells. Besides, these two mutations gave an incredibly high fluorescent intensities than the blank cells in $Dibac_3(4)$ assay, caused by an unknown reason. The flag tag inserted into the plasmid, in this case, can be utilized in channels trafficking to membrane surface. Furthermore, the relationship between MODY 12, 13 and other types may also give us some insights in how MODY mutations affecting the channel abilities.

References

Conditions, Genetic. "Maturity-Onset Diabetes of The Young: MedlinePlus Genetics". *Medlineplus.Gov*, 2022

American Diabetes Association Professional Practice Committee; 2. Classification and Diagnosis of Diabetes: Standards of Medical Care in Diabetes—2022. Diabetes Care 1 January 2022; 45 (Supplement_1): S17–S38.

Ashcroft, F. M., Harrison, D. E., & Ashcroft, S. J. (1984). Glucose induces closure of single potassium channels in isolated rat pancreatic β-cells. *Nature*, 312(5993), 446–448.

Nichols, C. KATP channels as molecular sensors of cellular metabolism. *Nature* 440, 470–476 (2006). https://doi.org/10.1038/nature04711

Noma, A. (1983). ATP-regulated K+ channels in cardiac muscle. *Nature*, 305(5930), 147–148. https://doi.org/10.1038/305147a0

Tinker, A., Aziz, Q., & Thomas, A. (2013). The role of ATP-sensitive potassium channels in cellular function and protection in the cardiovascular system. *British Journal of Pharmacology*, 171(1), 12–23. https://doi.org/10.1111/bph.12407

Jang K. M. (2020). Maturity-onset diabetes of the young: update and perspectives on diagnosis and treatment. *Yeungnam University journal of medicine*, 37(1), 13–21. https://doi.org/10.12701/yujm.2019.00409

Grange, D. K., Roessler, H. I., McClenaghan, C., Duran, K., Shields, K., Remedi, M. S., Knoers, N. V. A. M., Lee, J. M., Kirk, E. P., Scurr, I., Smithson, S. F., Singh, G. K., van Haelst, M. M., Nichols, C. G., & van Haaften, G. (2019). Cantú syndrome: Findings from 74 patients in the International Cantú Syndrome Registry. *American journal of medical genetics. Part C, Seminars in medical genetics,* 181(4), 658–681. https://doi.org/10.1002/ajmg.c.31753

Seino, S., & Miki, T. (2003). Physiological and pathophysiological roles of ATP-sensitive K+ channels. *Progress in Biophysics and Molecular Biology*, 81(2), 133–176. https://doi.org/10.1016/s0079-6107(02)00053-6

Loechner, K. J., Akrouh, A., Kurata, H. T., Dionisi-Vici, C., Maiorana, A., Pizzoferro, M., Rufini, V., de Ville de Goyet, J., Colombo, C., Barbetti, F., Koster, J. C., & Nichols, C. G. (2010). Congenital hyperinsulinism and glucose hypersensitivity in homozygous and heterozygous carriers of Kir6.2 (kcnj11) mutation V290M mutation. *Diabetes*, 60(1), 209–217. https://doi.org/10.2337/db10-0731

Yan, Z., Fortunato, M., Shyr, Z. A., Clark, A. L., Fuess, M., Nichols, C. G., & Remedi, M. S. (2022). Genetic reduction of glucose metabolism preserves functional β-cell mass in KATP-induced neonatal diabetes. *Diabetes*, 71(6), 1233–1245. https://doi.org/10.2337/db21-0992

Hamill, O. P., Marty, A., Neher, E., Sakmann, B., & Sigworth, F. J. (1981). Improved patch-clamp techniques for high-resolution current recording from cells and cell-free membrane patches. *Pflügers Archiv - European Journal of Physiology*, 391(2), 85–100. https://doi.org/10.1007/bf00656997

Melkikh, A. V., & Sutormina, M. I. (2008). Model of active transport of ions in cardiac cell. *Journal of Theoretical Biology*, 252(2), 247–254. https://doi.org/10.1016/j.jtbi.2008.02.006

Koganti, S.R. et al. (2015). Disruption of KATP channel expression in skeletal muscle by targeted oligonucleotide delivery promotes activity-linked thermogenesis, *Molecular Therapy*, 23(4), pp. 707–716. Available at: https://doi.org/10.1038/mt.2015.21.

Alekseev, A.E. et al. (2010) "Sarcolemmal ATP-sensitive K+ channels control energy expenditure determining body weight," *Cell Metabolism*, 11(1), pp. 58–69. Available at: https://doi.org/10.1016/j.cmet.2009.11.009.

Vedovato, N., Ashcroft, F. M., & Puljung, M. C. (2015). The Nucleotide-Binding Sites of SUR1: A Mechanistic Model. *Biophysical journal*, 109(12), 2452–2460. https://doi.org/10.1016/j.bpj.2015.10.026

Saint-Martin, C. et al. (2011). KATP channel mutations in congenital hyperinsulinism, *Seminars in Pediatric Surgery*, 20(1), pp. 18–22. Available at: https://doi.org/10.1053/j.sempedsurg.2010.10.012.

Ashcroft, F.M., Harrison, D.E. and Ashcroft, S.J. (1984). Glucose induces closure of single potassium channels in isolated rat pancreatic β-cells, *Nature*, 312(5993), pp. 446–448. Available at: https://doi.org/10.1038/312446a0.

Ashcroft, F.M. (2005). ATP-sensitive potassium channelopathies: Focus on insulin secretion, *Journal of Clinical Investigation*, 115(8), pp. 2047–2058. Available at: https://doi.org/10.1172/jci25495.

De Franco, E., Saint-Martin, C., Brusgaard, K., Knight Johnson, A. E., Aguilar-Bryan, L., Bowman, P., Arnoux, J. B., Larsen, A. R., Sanyoura, M., Greeley, S. A. W., Calzada-León, R., Harman, B., Houghton, J. A. L., Nishimura-Meguro, E., Laver, T. W., Ellard, S., Del Gaudio, D., Christesen, H. T., Bellanné-Chantelot, C., & Flanagan, S. E. (2020). Update of variants identified in the pancreatic β-cell KATP channel genes KCNJ11 and ABCC8 in individuals with congenital hyperinsulinism and diabetes. *Human mutation*, 41(5), 884–905. https://doi.org/10.1002/humu.23995

Cooper, P. E., McClenaghan, C., Chen, X., Stary-Weinzinger, A., & Nichols, C. G. (2017). Conserved functional consequences of disease-associated mutations in the slide helix of Kir6.1 and Kir6.2 subunits of the ATP-sensitive potassium channel. *The Journal of biological chemistry*, 292(42), 17387–17398. https://doi.org/10.1074/jbc.M117.804971

Pipatpolkai, T. et al. (2020). New insights into KATP channel gene mutations and neonatal diabetes mellitus, *Nature Reviews Endocrinology*, 16(7), pp. 378–393. Available at: https://doi.org/10.1038/s41574-020-0351-y.

Ashcroft, F.M., Puljung, M.C. and Vedovato, N. (2017). Neonatal diabetes and the K ATP channel: From mutation to therapy, *Trends in Endocrinology & Metabolism*, 28(5), pp. 377–387. Available at: https://doi.org/10.1016/j.tem.2017.02.003.

Şıklar, Z. et al. (2011). Transient neonatal diabetes with two novel mutations in the KCNJ11 gene and response to sulfonylurea treatment in a preterm infant, *Journal of Pediatric Endocrinology and Metabolism*, 24(11-12). Available at: https://doi.org/10.1515/jpem.2011.250.

Thomas, P. M., Cote, G. J., Wohllk, N., Haddad, B., Mathew, P. M., Rabl, W., Aguilar-Bryan, L., Gagel, R. F., & Bryan, J. (1995). Mutations in the sulfonylurea receptor gene in familial persistent hyperinsulinemic hypoglycemia of infancy. *Science*, 268(5209), 426–429. https://doi.org/10.1126/science.7716548

Nichols CG, Shyng SL, Nestorowicz A, Glaser B, Clement JP 4th, Gonzalez G, Aguilar-Bryan L, Permutt MA, Bryan J. Adenosine diphosphate as an intracellular regulator of insulin secretion. *Science*. 1996 Jun 21;272(5269):1785-7. doi: 10.1126/science.272.5269.1785. PMID: 8650576.

Boodhansingh, K.E. et al. (2019). Novel dominant KATP channel mutations in infants with congenital hyperinsulinism: Validation by in vitro expression studies and in vivo carrier phenotyping, *American Journal of Medical Genetics Part A*, 179(11), pp. 2214–2227. Available at: https://doi.org/10.1002/ajmg.a.61335.

Pinto, D. L., De Araújo, R., Cruz, S. A., Canavarro, T. A., & Brito, M. A. (2021). Diabetes monogênico: Diabetes tipo mody, diabetes neontal / monogenic diabetes: Mody diabetes, neonatal diabetes. *Brazilian Journal of Development*, 7(12), 114188–114205. https://doi.org/10.34117/bjdv7n12-276

Horikawa Y. (2018). Maturity-onset diabetes of the young as a model for elucidating the multifactorial origin of type 2 diabetes mellitus. *Journal of diabetes investigation*, 9(4), 704–712. https://doi.org/10.1111/jdi.12812

Biolabs, N.E. Q5® high-fidelity DNA polymerases, NEB. Available at: https://www.neb.com/products/pcr-qpcr-and-amplification-technologies/q5-high-fidelity-dna-polymerases/q5-high-fidelity-dna-polymerases?gclid=Cj0KCQiA1ZGcBhCoARIsAGQ0kkp4Unafris86byn1-id-HGW0h8y_DMfABEaNfbdO2ZZd3y72bWUXswaAkJGEALw_wcB.

Kommedal, Ø., Simmon, K., Karaca, D., Langeland, N., & Wiker, H. G. (2012). Dual priming oligonucleotides for broad-range amplification of the bacterial 16S rRNA gene directly

from human clinical specimens. *Journal of clinical microbiology*, 50(4), 1289–1294. https://doi.org/10.1128/JCM.06269-11

SOC medium for use in Transformation: Sigma-aldrich (no date) Sigma. Available at: https://www.sigmaaldrich.com/US/en/product/sigma/s1797.

Bicistronic or internal ribosome entry site (IRES) element - efficient co-expression of two genes in a single vector (no date) Genecopoeia. Available at: https://www.genecopoeia.com/tech/ires/#:~:text=IRES%20enables%20the%20coordinated%20co,it%20with%20the%20same%20vector.

Biolabs, N.E. RCutSmart™ buffer, NEB. Available at: https://www.neb.com/products/b6004-rcutsmart-buffer#Product%20Information.

Qiaprep Spin Miniprep Kit. QIAGEN. Available at: https://www.qiagen.com/us/products/discovery-and-translational-research/dna-rna-purification/dna-purification/plasmid-dna/qiaprep-spin-miniprep-kit/.

Adams, D. S., & Levin, M. (2012). General principles for measuring resting membrane potential and ion concentration using fluorescent bioelectricity reporters. *Cold Spring Harbor protocols,* 2012(4), 385–397. https://www.ncbi.nlm.nih.gov/pmc/articles/PMC4001120/

Hansen, J. (2006). Towards selective kir6.2/sur1 potassium channel openers, Medicinal Chemistry and Therapeutic Perspectives. *Current Medicinal Chemistry*, 13(4), 361–376. https://doi.org/10.2174/092986706775527947

Brayden, J. E. (2002). Functional roles of KATP channels in vascular smooth muscle. *Clinical and Experimental Pharmacology and Physiology*, 29(4), 312–316. https://doi.org/10.1046/j.1440-1681.2002.03650.x

Hudman, D., Elliott, R. A., & Norman, R. I. (2000). KATP channels mediate the β2-adrenoceptor agonist-induced relaxation of rat detrusor muscle. *European Journal of Pharmacology*, 397(1), 169–176. https://doi.org/10.1016/s0014-2999(00)00229-6

Matreyek, K. A., et al. (2020). An improved platform for functional assessment of large protein libraries in mammalian cells. *Nucleic Acids Res,* 48(1): e1.

Maiorana, A., Barbetti, F., Boiani, A., Rufini, V., Pizzoferro, M., Francalanci, P., Faletra, F., Nichols, C. G., Grimaldi, C., de Ville de Goyet, J., Rahier, J., Henquin, J.-C., & Dionisi-Vici, C. (2014). Focal congenital hyperinsulinism managed by medical treatment: A diagnostic algorithm based on molecular genetic screening. *Clinical Endocrinology*, 81(5), 679–688. https://doi.org/10.1111/cen.12400

Remedi, M. S., Kurata, H. T., Scott, A., Wunderlich, F. T., Rother, E., Kleinridders, A., Tong, A., Brüning, J. C., Koster, J. C., & Nichols, C. G. (2009). Secondary consequences of β cell inexcitability: Identification and prevention in a murine model of KATP-induced neonatal

diabetes mellitus. *Cell Metabolism*, 9(2), 140–151.
https://doi.org/10.1016/j.cmet.2008.12.005

Işık, E. et al. (2019). Congenital hyperinsulinism and evolution to sulfonylurearesponsive diabetes later in life due to a novel homozygous p.L171F abcc8 mutation, *Journal of Clinical Research in Pediatric Endocrinology*, 11(1), pp. 82–87. Available at: https://doi.org/10.4274/jcrpe.galenos.2018.2018.0077.

Kharade, S. V., Nichols, C., & Denton, J. S. (2016). The shifting landscape of Katpchannelopathies and the need for 'sharper' therapeutics. *Future Medicinal Chemistry*, 8(7), 789–802. https://doi.org/10.4155/fmc-2016-0005